Early antiviral CD4 and CD8 T cell responses and antibodies are associated with upper respiratory tract clearance of SARS-CoV-2

Sydney I. Ramirez[1, 2], Paul G. Lopez[1], Farhoud Faraji[1,3], Urvi M. Parikh[4], Amy Heaps[4], Justin Ritz[5], Carlee Moser[5], Joseph J. Eron[6], David A. Wohl[7], Judith S. Currier[7], Eric S. Daar[8], Alex L. Greninger[9], Paul Klekotka[10], Alba Grifoni[1], Daniela Weiskopf[1,2], Alessandro Sette[1,2], Bjoern Peters[1,2], Michael D. Hughes[5], Kara W. Chew[7], Davey M. Smith[2†], and Shane Crotty[1,2†], for the ACTIV-2/A5401 Study Team

[1]Center for Vaccine Innovation, La Jolla Institute for Immunology, La Jolla, CA, USA
[2]University of California San Diego, Department of Medicine, Division of Infectious Diseases and Global Public Health, La Jolla, CA, USA
[3]University of California San Diego, Department of Otolaryngology-Head and Neck Surgery, La Jolla, CA, USA
[4]Division of Infectious Diseases, Department of Medicine, University of Pittsburgh School of Medicine, Pittsburgh, PA, USA
[5]Center for Biostatistics in AIDS Research, Harvard T.H. Chan School of Public Health, Boston, MA, USA
[6]Department of Medicine, University of North Carolina at Chapel Hill School of Medicine, Chapel Hill, NC, USA
[7]Division of Infectious Diseases, Department of Medicine, David Geffen School of Medicine at University of California, Los Angeles, Los Angeles, CA, USA
[8]Lundquist Institute at Harbor-UCLA Medical Center, Torrance, CA, USA
[9]Department of Laboratory Medicine and Pathology, University of Washington Medical Center, Seattle, WA, USA
[10]Eli Lilly and Company, San Diego, CA, USA

[†]Correspondence:
Shane Crotty, 9420 Athena Circle, La Jolla, CA, 92037, +1 858-752-6500, shane@lji.org; Davey M. Smith, 9500 Gilman Drive #0679, La Jolla, CA, 92093, +1 858-642-1620, d13smith@health.ucsd.edu.

Running title: Early T cell responses to SARS-CoV-2 associated with upper airway viral clearance

Conflict-of-interest J.S.C. has consulted for Merck and Company. A.L.G. reports contract testing from Abbott, Cepheid, Novavax, Pfizer, Janssen and Hologic and research support from Gilead, outside of the described work. P.K. is an employee and shareholder of Eli Lilly. D.W. is a consultant for Moderna. A.S. is a consultant for AstraZeneca Pharmaceuticals, Calyptus Pharmaceuticals, Inc, Darwin Health, EmerVax, EUROIMMUN, F. Hoffman-La Roche Ltd, Fortress Biotech, Gilead Sciences, Gritstone Oncology, Guggenheim Securities, Moderna, Pfizer, RiverVest Venture Partners, and Turnstone Biologics. K.W.C. has received research funding to the institution from Merck Sharp & Dohme. D.M.S. has consulted for and has equity stake in Linear Therapies, Model Medicines and Vx Biosciences and consulted for Bayer, Kiadis, Signant Health and Brio Clinical. S.C. has consulted for GSK, JP Morgan, Citi, Morgan Stanley, Avalia NZ, Nutcracker Therapeutics, University of California, California State Universities, United Airlines, Adagio, and Roche. LJI has filed for patent protection for various aspects of T cell epitope and vaccine design work. The other authors have no competing interests to declare.

ABSTRACT

T cells are involved in protective immunity against numerous viral infections. Data regarding functional roles of human T cells in SARS-CoV-2 (SARS2) viral clearance in primary COVID-19 are limited. To address this knowledge gap, samples were assessed for associations between SARS2 upper respiratory tract viral RNA levels and early virus-specific adaptive immune responses for 95 unvaccinated clinical trial participants with acute primary COVID-19 aged 18-86 years old, approximately half of whom were considered high risk for progression to severe COVID-19. Functionality and magnitude of acute SARS2-specific CD4 and CD8 T cell responses were evaluated, in addition to antibody responses. Most individuals with acute COVID-19 developed SARS2-specific T cell responses within 6 days of COVID-19 symptom onset. Early CD4 T cell and CD8 T cell responses were polyfunctional, and both strongly associated with reduced upper respiratory tract SARS2 viral RNA, independent of neutralizing antibody titers. Overall, these findings provide evidence for protective roles for circulating SARS2–specific CD4 and CD8 T cells during acute COVID-19.

MAIN

Introduction

Since the emergence of severe acute respiratory syndrome coronavirus 2 (SARS2) as a novel human pathogen, much has been learned about protective immunity to SARS2, both in the context of infection and COVID-19 vaccines. Serologic correlates of protection have been established for vaccines (1–8). In the context of prophylaxis, virus neutralization by monoclonal antibodies (mAb) has been demonstrated as one mechanism of protective immunity (9–12). In contrast, in the context of infection the relative importance of immune system compartments may differ, due to the substantial differences in kinetics of primary versus memory immune responses and lack of pre-existing antibodies. Studies of primary adaptive immunity to acute SARS2 infection offer a key opportunity to evaluate early humoral and cellular immune responses and their individual contributions to protection.

The global population rapidly developed widespread cellular and humoral immunity to SARS2 as a result of both vaccination and infection. However, key gaps in our understanding of human primary immune responses to SARS2 remain. Cellular immunity may be required for viral control and clearance during acute infection (13–17). While acute and memory T cell responses clearly occur to SARS2 infection (18–24) and COVID-19 vaccines (25–32), evidence of functional protective roles of T cells have been limited in humans (16, 33), particularly by assessing non-hospitalized COVID-19 cases (34–36). Due to the combined difficulties of identifying early acute COVID-19 cases, recruiting those individuals, and the technical challenges of measuring virus-specific T cell responses and viral loads concomitantly, most acute T cell studies have been limited to small cohorts, including hospitalized cases, sometimes relatively late in disease, and often without viral load measurements (22, 37–40). In a controlled SARS-CoV-2 human challenge study of young adults with a mean age of 22 years old, early circulating SARS2-specific CD8 T cells were associated with SARS2 viral clearance in that cohort of 18 subjects (36). There is evidence for cellular immunity contributing to SARS2 protection in non-human primate models (16, 17). Breakthrough infections represent a different context for studying protective immunity in humans, in which there is

evidence for contributions of memory T cells (41, 42). Given expanded interest in next-generation COVID-19 and pan-sarbecovirus vaccines with T cell-specific components (43, 44), or vaccines that are entirely T cell-based (30, 45, 46), future vaccine designs and clinical trial designs would benefit from better fundamental understanding of T cell protective immunity to COVID-19 in humans (30, 34).

Results

Longitudinal data were collected for 95 individuals with primary SARS2 infection in 2020, prior to the availability of COVID-19 vaccines, with sampling including nasopharyngeal (NP) swabs for SARS2 RNA, serum, and peripheral blood mononuclear cells (PBMCs), all collected in the context of a randomized, controlled clinical trial (ACTIV-2/A5401, NCT04518410). Herein, serum antibodies, SARS2-specific CD4 T cell, and SARS2-specific CD8 T cell response measurements are reported, which is the largest and most comprehensive acute viral and antigen-specific immune response data set of its kind.

All participants were enrolled within 7 days from positive SARS2 testing and 10 days from COVID-19 symptom onset (21, 47). Individuals studied herein were among those randomized to receive either 700 mg of the mAb bamlanivimab or placebo (saline) intravenously (**Fig. 1A**) on study day 0 (median of 6 days post-symptom onset; **Fig. 1B**). The 46 bamlanivimab treatment and 49 placebo subjects were similar with respect to baseline characteristics such as age, biological sex at birth, risk for progression to severe COVID-19, and time post-symptom onset at randomization (**Fig. 1A and S1A**, and ref (21, 47)). Peripheral blood was collected prior to mAb or placebo administration on study day 0. NP swabs were collected from all 95 participants by trained study staff prior to treatment on study day 0, with SARS2 viral RNA was detectable in the NP swabs of nearly all individuals (89%) (**Fig. 1C**), and no significant difference in SARS2 NP RNA between the bamlanivimab (treatment) and placebo groups (**Fig. S1B**). SARS2 NP RNA at study day 0 was not associated with participant age ($r = 0.16$, $p = 0.12$, **Fig. S1C**). SARS2 NP RNA levels declined over time (**Fig. 1D**), as expected (48–50), and as previously reported for the full ACTIV-2/A5401 cohort (47).

Both NP swab and peripheral blood samples were collected prior to treatment on study day 0. Acute adaptive immune responses were measured for all participants prior to treatment. Additionally, longitudinal responses were measured in the 49 placebo group participants post-treatment on study days 7 and 28. We previously reported day 28 antibody, memory CD4 T cell, and memory CD8 T cell outcomes (21). Early (study day 0) SARS2-specific CD4 T cell response magnitude and functionality were evaluated by multiple techniques and using multiple SARS2 antigens. Activation induced marker (AIM), and hybrid AIM plus intracellular cytokine staining (AIM+ICS) T cell assays were employed (**Fig. 2A-B**, **Fig. S2A**). SARS2 Spike (S)- and non-Spike-specific CD4 T cells were measured by AIM assays following stimulation with S and non-S (CD4-RE (ref 28)) peptide megapools (MP). Two sets of AIM phenotyping surface protein marker pairs were utilized to assign AIM assay positivity (expression of surface $OX40^+$ and $41BB^+$, **Fig. 2A**, and surface $OX40^+$ and $CD40L^+$, **Fig. S2B**). SARS2-specific CD4 T cell frequencies were comparable by AIM based on $OX40^+41BB^+$ or $OX40^+CD40L^+$ surface marker expression (**Fig. 2A and S2B**). Seventy-seven percent of individuals were positive for S-specific CD4 T cells, and 79% of individuals were positive for non-S CD4 T cells (**Fig. 2A**). Combined responses to SARS2 S- and non-S epitopes were also quantified to evaluate total antiviral T cell responses per subject (**Fig. 2A and S2B. Fig. S2C-G**). Overall, substantial CD4 T cell responses were observed.

123 SARS2-specific CD4 T cells were phenotyped based on cytokine production by ICS following
124 stimulation with the S and non-S MPs, including interferon gamma (IFNγ), granzyme B (GzmB), tumor
125 necrosis factor (TNF), and interleukin-2 (IL-2) production by CD40L$^+$ CD4 T cells (**Fig. 2B-F and S2H-J**).
126 IFNγ was the most expressed cytokine at study day 0 (**Fig. 2B**) and is known to be important in control of
127 multiple viral infections in mouse models. Between 85-87% of individuals had SARS2–specific CD4 T cell
128 responses by AIM or IFNγ ICS (combined S plus non-S responses; **Fig. 2A-B**). SARS2-specific CD4 T cells
129 were polyfunctional, with 69% producing at least 2 cytokines, and 53% producing 3 or more cytokines
130 (**Fig. 2B-F**). SARS2-specific circulating T follicular helper cells (cT_{FH}, CXCR5$^+$) were measured. Similar
131 response rates were seen for SARS2-specific cT_{FH} as for total SARS2-specific CD4 T cells. SARS2-specific
132 circulating T_{FH} cells were observed in 79-84% of participants' study day 0 PBMC (**Fig. 2G-H**). Overall,
133 SARS2-specific CD4 T cells with different functionalities and differentiation states were present.
134 In parallel, study day 0 SARS2 S- and non-S-specific CD8 T cell responses were evaluated by AIM
135 (surface CD69$^+$41BB$^+$) and ICS following stimulation with SARS2 S and non-S (CD8-RE (ref 28)) MPs (**Fig.**
136 **S3A, D-F**). Acute SARS2–specific CD8 T cell responses were observed at study day 0 in 63% of individuals
137 by AIM (**Fig. S3B**). By ICS, 62% of individuals were positive for an acute SARS2–specific CD8 T cell
138 response (surface CD69$^+$ and intracellular IFNγ$^+$, **Fig. 3A**). As was observed for SARS2-specific CD4 T cells,
139 IFNγ was the cytokine most commonly produced by SARS2-specific CD8 T cells (**Fig. 3A**). CD8 ICS was
140 used as the primary quantification of SARS2-specific CD8 T cells in downstream analyses given the similar
141 detection rates of antigen-specific CD8 T cells but lower background for the CD69$^+$IFNγ$^+$ CD8 T cell assay
142 (**Fig. 3A** LOQ) compared to CD8 AIM (**Fig. S3B** LOQ) (see Methods for additional details). As expected,
143 CD8 T cell responses did not vary on study day 0 when assessed by clinical trial group assignment (**Fig.**
144 **S3C**). Most CD69$^+$ IFNγ-producing SARS2-specific CD8 T cells also produced GzmB (73%, **Fig. 3B and**
145 **S3D**). Similar to SARS2-specific CD4 T cells, SARS2-specific CD8 T cells were predominantly
146 polyfunctional, with 69% producing at least 2 cytokines and 58% producing 3 or more cytokines (**Fig. 3A-**
147 **E**). Overall, polyfunctional virus-specific CD4 and CD8 T cell responses were detected in a substantial
148 proportion of individuals during acute primary SARS2 infection.
149 We examined the kinetics of T cell and antibody responses in the placebo group in more detail.
150 Longitudinal assessment of SARS2-specific CD4 and CD8 T cell frequencies on study days 0 (**Fig. 2-3**), 7
151 (**Fig. 4A-C and S4A**), and 28 (**Fig. 4A-C, S4A**, and ref.(21)) showed that AIM$^+$ CD4 T cell frequencies and
152 the proportion of positive responders increased over time (**Fig. 4A and S4A**). SARS2-specific IFNγ$^+$ CD4
153 and CD8 T cell frequencies remained stable from study days 0 to 28 (**Fig. 4B-C**), suggesting that antigen-
154 specific IFNγ-producing T cells are formed early during primary infection and stably maintained at least
155 through early convalescence. SARS2 serologic assessments, included nAb titers to ancestral SARS2 by
156 lentiviral pseudovirus neutralization assays (PSV NT50) and receptor binding domain (RBD) binding IgG
157 titers measured on study day 0 (**Fig. 4D-E** and ref 21 for RBD IgG). Most individuals were found to have
158 formed nAb to SARS2 within 6 days post-COVID symptom onset. On study day 0, 62% of participants had
159 positive nAb titers (**Fig. 4D, Fig. 4SB**). As expected, nAb and RBD IgG titers increased between study days
160 0 and 7 (**Fig. S4D-E**).
161 To evaluate potential protective activities of early T cell responses, associations were examined
162 between study day 0 NP viral RNA levels and the magnitude and diversity of SARS2–specific CD4 and
163 CD8 T cell responses. The presence and magnitude of early SARS2-specific CD4 T cell responses were

164 associated with lower levels of SARS2 NP RNA based on all three main CD4 T cell measurements of
165 activation ($OX40^+41BB^+$ AIM Spearman r = -0.51, p = $2.6x10^{-7}$, **Fig. 5A**; $OX40^+CD40L^+$ AIM r = -0.45, p =
166 $9.3X10^{-6}$, **Fig. S5A**) and IFNγ production ($CD40L^+IFN\gamma^+$, r = -0.36, p = $5x10^{-4}$, **Fig. 5B**). Early SARS2-specific
167 CD8 T cell response magnitude and IFNγ production were also associated with lower levels of SARS2 NP
168 RNA ($IFN\gamma^+$ r = -0.44, p = $1.1x10^{-5}$, **Fig. 5C**; $CD69^+41BB^+$ AIM r = -0.39, p = $1.4x10^{-4}$, **Fig. S5C**). SARS2-
169 specific T cell and SARS2 NP RNA associations were strongest when using combined S plus non-S T cell
170 response measurements. Statistical associations were similar when S and non-S antigen-specific responses
171 were evaluated separately, though generally stronger for non-S than S-specific responses (**Fig. S5D-J**). A
172 positive correlation was observed between total SARS2-specific CD4 and CD8 T cell responses (**Fig. S5K**).
173 A positive correlation was also observed between day 0 nAb and RBD IgG titers (**Fig. S5L**), as expected[48].
174 Notably, SARS2 nAb titers measured at study day 0 were also associated with lower levels of SARS2 NP
175 RNA, but the association with nAb was weaker than the association with either day 0 SARS2-specific CD4
176 or CD8 T cells (r = -0.33, p = $1.2x10^{-3}$, **Fig. 5D**).
177 Given the biological dependence of the antibody response on CD4 T cell help mediated by T_{FH}
178 cells (51, 52), some statistical association between antibodies and viral load would always be expected,
179 even if, hypothetically, viral control was exclusively mediated by T cells. Early S-specific cT_{FH} cells had
180 relatively modest associations with SARS2 NP RNA that were weaker than total S-specific CD4 T cell AIM
181 response associations but similar to nAb titer associations (Spearman r = -0.37 to 0.39, p = 1.6 to 2.8 $x10^{-}$
182 ^{4} , **Fig. S5I-J**). Analysis of covariance (ANCOVA) testing was performed to better evaluate if the putative
183 protective relationships observed between early SARS2-specific CD4 T cell responses and SARS2 NP RNA
184 remained after accounting for antibodies, based on day 0 nAb serostatus. Associations between total
185 SARS2-specific CD4 or SARS2-specific cT_{FH} T cell responses and lower SARS2 NP RNA did not show a
186 dependence on SARS2 nAb seropositivity (**Fig. S5M-O**). SARS2-specific CD8 T cell associations with lower
187 SARS2 NP RNA was also independent of nAb seropositivity (**Fig. S5M**). Thus, early SARS2–specific CD4
188 and CD8 T cell responses were specifically associated with reduced upper airway SARS2 viral loads in
189 unvaccinated, non-hospitalized cases of acute COVID-19.
190 Examining SARS2 antigen-specific CD4 and CD8 cytokine production and associations with viral
191 NP RNA at study day 0 revealed that in addition to IFNγ production, production of the Th1 cytokines
192 GzmB, IL-2, and TNF similarly correlated with lower NP viral RNA levels (**Fig. S6A-F**). These associations
193 were similar for cytokine-producing CD4 and CD8 T cells recognizing both Spike and non-Spike epitopes.
194 SARS2-specific CD4 T cells, associations were similar regardless of which cytokine the cells were
195 producing, but for SARS2-specific CD8 T cells production of both IFNγ and GzmB was most strongly
196 associated with decreased SARS2 NP RNA (**Fig. S6D**). Thus, diverse and polyfunctional SARS2-specific
197 CD4 and CD8 T cell responses, including CD4 and CD8 T cells with profiles of cytotoxicity, may play a role
198 in viral clearance during acute SARS-CoV-2 primary infection.
199 Participants in the study enrolled at a range of days post-symptom onset (PSO), which provides
200 richness to the dataset, but raised the possibility that the immune response associations with reduced NP
201 viral RNA levels might only be surrogates for time from infection. To test this possibility, an analysis was
202 performed to try to account for differences in time from symptom onset to study entry, using simple log-
203 linear regression models of the raw data to extrapolate SARS2-specific immune response and NP RNA
204 data to day 6 PSO (the median number of days PSO for all participants) (**Fig. S7A-E**, see Methods). If the

205 original SARS2-specific T cell associations with reduction of SARS2 NP RNA levels were only surrogates of
206 time from infection (measured as days PSO), T cell associations should be lost upon adjustment for days
207 PSO. If instead the T cell associations reflected a functional relationship, statistical associations between T
208 cell responses and lower viral RNA would be expected to remain after adjustment for days PSO. Although
209 weaker, the relationships between CD4 and CD8 T cell responses and viral NP RNA levels adjusted to 6
210 days PSO remained statistically significant (CD4 AIM r = -0.39, p = 1.9×10^{-4} **Fig. S7F**; CD4 IFNγ^{+} r = -0.35,
211 p = 1.0×10^{-3} **Fig. S7G**; CD8 IFNγ^{+} r = -0.31, p = 4.4×10^{-3} **Fig. S7H**), consistent with a functional role for T
212 cells in control of viral NP RNA levels. Associations between nAb titers and viral NP RNA levels also
213 remained after adjustment (r = -0.32, p = 3.0×10^{-3} **Fig. S7I**). Altogether, these data are evidence of
214 functional relationships in humans between the development of early antiviral CD4 and CD8 T cell
215 responses, and antibodies, and control of acute SARS2 infection in the upper airway.
216 In summary, this study provides new insights into the relationship between acute adaptive immune
217 responses to SARS2 and viral control. It has been hypothesized that SARS2–specific antiviral T cell
218 responses may contribute to protection from symptomatic and severe disease by reducing viral burden
219 and the enhancing speed of viral clearance; however, few human studies have directly measured the role
220 of cellular immunity on viral control of primary infection (36, 40). Here, using samples from 95 individuals
221 who participated in a randomized, controlled clinical trial, the largest virus-specific acute immune response
222 data set of its kind was generated for adults up to 86 years of age, including many subjects at risk for
223 progression to severe COVID-19.
224

225 ## Discussion

226 The data demonstrate that (i) SARS2-specific CD4 and CD8 T cells could be detected in the majority of
227 adults with outpatient COVID-19 within days from symptom onset, (ii) the T cells were polyfunctional, (iii)
228 stronger early SARS2-specific CD4 T cell responses were associated with lower viral RNA levels in the
229 upper airway, (iv) stronger SARS2-specific CD8 T cell responses were associated with lower viral RNA levels
230 in the upper airway, (v) the associations of T cell responses with lower viral RNA were independent of
231 neutralizing antibody responses and (vi) remained significant after accounting for time from COVID-19
232 symptom onset. The conclusions from these analyses of T cell associations with viral control were
233 reproducible by multiple different measurements of CD4 T cell and CD8 T cell functionalities and SARS2
234 antigen specificities. Overall, these findings suggest that SARS2–specific T cells play a role in protective
235 immunity to SARS2 during acute infection.
236 In a smaller study (n=25 acute infections sampled), Eser *et al.* found a strong association between
237 nucleocapsid-specific IFNγ^{+} CD4 T cells and lower viral loads (40). Those results are consistent with the
238 CD4 T cell findings here, except the findings here were that T cell responses to S or non-S antigens were
239 both associated with reduced viral loads and were approximately equally associated with reduced viral
240 loads though somewhat higher for non-S responses. Eser *et al.* observed less of an association for
241 nucleocapsid-specific IFNγ^{+} CD8 T cell responses and lower viral loads, perhaps because the study sample
242 size was limited and fewer participants developed early circulating nucleocapsid-specific IFNγ^{+} CD8 than
243 CD4 T cell responses (40).
244 In a human controlled SARS2 infection study of healthy young adults (n=18 infected. Mean age of
245 22 years old) with a limited infectious dose (53% of individuals were infected), total CD38^{+}Ki67^{+} CD8 T

246 cells in peripheral blood were the strongest association with accelerated viral clearance (36). Those data
247 are consistent with the CD8 T cell findings here regarding early SARS2-specific CD8 T cell activation being
248 associated with reduced viral NP RNA. A strength of that study was the precisely defined time of infection
249 and longitudinal tracking of viral loads and T cell responses in blood based on markers. Several factors
250 distinguish the study reported herein. Early SARS2 Spike- and non-Spike-specific CD8 T cells both
251 correlated with viral clearance, including when quantified by two different T cell assays (AIM and/or IFNγ
252 production). Additionally, early SARS2 total, S- and non-S-specific CD4 T SARS2-specific responses also
253 correlated. Furthermore, SARS2-specific cT_{FH} were also associated with lower viral loads herein. The cohort
254 size here is substantially larger (95 compared to 18) and presumably includes subjects infected by a range
255 of viral exposure doses. The virus-specific T cell assays herein measured CD4 and CD8 T cell epitopes
256 spanning the Spike protein and non-S antigens including both structural and non-structural proteins and
257 we were able to detect early circulating SARS2-specific T cells. Given that non-structural proteins are
258 expressed earlier in infection and are better conserved across human coronaviruses, it is possible that the
259 inclusion of non-structural protein epitopes in our peptide megapools allows for earlier and more
260 comprehensive detection of both cross-reactive and SARS2-specific circulating T cell responses than
261 peptide pools containing only SARS-CoV-2 structural protein epitopes (38, 53, 54). Additionally, the data
262 herein demonstrate that the early SARS2-specific CD4 and CD8 T cells were polyfunctional, not only
263 defined by IFNγ production (36, 40). Lastly, in the controlled infection study (36) all subjects were young
264 healthy adults (mean age 22 years old), while the subjects herein were from a broad age range (18-86
265 years old) and half had comorbid conditions considered to be high risk for development of severe COVID-
266 19. Thus, the data herein represent a broad age spectrum and are also particularly relevant for those age
267 groups and demographics most at risk for worse outcomes due to COVID-19 like hospitalization or death.
268 This study in no way excludes a complementary role for antibodies in control of SARS2 in
269 unvaccinated individuals. Our study has limitations. It is intrinsically challenging to disentangle roles of T
270 cells from roles of antibodies in combatting SARS2 in humans (15, 17, 18). This study provides evidence
271 that SARS2-specific T cell responses exhibit selective correlates with viral clearance, but it is entirely
272 plausible that coordinated adaptive immunity of T cells and antibodies are important in protection (14, 16,
273 39). Additionally, adaptive immune responses at the site of initial infection were not directly assessed in
274 this study and may not be adequately captured by evaluation of circulating immune cells and antibodies
275 from peripheral blood samples. Thus, a role for local, upper airway cellular and humoral immunity in
276 protection from SARS2 cannot be excluded (16, 36, 55–57). The study was also underpowered to
277 distinguish the myriad roles that different CD4 and CD8 T cell subsets may individually play in viral
278 clearance, or to determine whether SARS2-specific CD4 and CD8 T cell responses are independent. We
279 were able to demonstrate that associations between early SARS2-specific CD4 and CD8 T cell responses
280 and NP viral RNA were independent of both nAb serostatus and time from SARS2 infection using relatively
281 simple statistical models. While this is in agreement with other studies demonstrating a role for T cells
282 protection against SARS2 infection (36, 39, 40), the use of more sophisticated mathematical models
283 applied across multiple data sets may provide additional insight. Lastly, our findings focused on primary
284 infection with ancestral SARS2 and may not be reflective of all individuals with acute COVID-19, including
285 primary infection by SARS2 variants or SARS2 breakthrough infections.
286 While T cell kinetics and phenotypes in response to SARS2 infection and COVID-19 vaccination

287 may not be identical and are shaped by exposure history (28, 41, 58), the cumulative data now indicate
288 that SARS2-specific T cells appear to play a protective role in both primary SARS2 infection and
289 breakthrough infections. It has been observed that in COVID-19 vaccinated individuals who experience
290 breakthrough infections, recall responses include rapid activation of memory S-specific CD4 and CD8 T
291 cells within the first week, which precede humoral responses, and that S-specific CD8 T cells are associated
292 accelerated viral clearance (41, 42). Given the overall findings in the field, next generation SARS2 or pan-
293 sarbecovirus vaccines may benefit from eliciting enhanced T cell responses, and from clinical trials that
294 assess both baseline and vaccination-induced SARS2-specific CD4 and CD8 T cell responses and
295 functionality.
296
297

298 ## METHODS

299 ### Sex as a biological variable

300 Our study examined similar numbers of males and females as SARS-CoV-2 infects both males
301 and females (**Fig. 1A**). Similar findings are reported for both males and females.
302

303 ### Study population and trial

304 ACTIV-2/A5401 was a multicenter phase 2/3 randomized controlled trial designed to evaluate the safety
305 and antiviral and clinical efficacy of therapeutics for acute COVID-19 in non-hospitalized adults. Individuals
306 in this study represent a subset of participants from ACTIV-2/A5401 who received a single intravenous
307 dose of 700 mg of bamlanivimab or normal saline placebo (comparator control group) and had available
308 clinical data (e.g., demographics, days post-symptom onset, risk for severe COVID-19; **Fig. 1A** and ref(21,
309 47)) and blood samples for immunologic testing. Samples from nearly half of the overall bamlanivimab 700
310 mg and comparator placebo groups were available for this study. Participants were from the United States
311 and enrolled in ACTIV-2/A5401 between October-November 2020. At study entry, COVID-19 vaccines
312 were not available to the general population in the United States and SARS2 infections could be attributed
313 to ancestral SARS2 virus. The subjects in this study were comparable at study entry across treatment
314 groups (**Fig. 1A** and ref(21, 47)). Inclusion criteria for ACTIV-2/A5401 included adults 18 years or older
315 with no more than 10 days of COVID-19 symptoms and documented SARS2 infection by FDA-authorized
316 antigen or molecular testing within seven days prior to study entry. Subjects were assigned to the
317 bamlanivimab or placebo groups at a 1:1 ratio, and randomization was stratified by time from symptom
318 onset (less than or ≥5 days post-symptom onset) and risk of progression to severe COVID-19 based on
319 age (less than or ≥ 55 years old) and the presence or absence of pre-defined comorbid medical conditions
320 (e.g., body mass index > 35kg/m^2, hypertension, diabetes) (47). Additional information for ACTIV-2/A5401
321 is available at ClinicalTrials.gov (Identifier: NCT04518410) and in the primary outcomes manuscript (47).
322 Three individuals were noted to have high NP viral loads despite high nAb titers at study day 0 (**Fig. 5D**).
323 Notably, one of these three individuals was in the placebo group. It was subsequently re-confirmed that
324 blood was drawn for all participants prior to bamlanivimab or placebo infusion, and that none of the
325 placebo group participants received bamlanivimab or any other active drug treatment for COVID-19.
326 Partial data for day 0 RBD IgG titers by group, similar to the data shown in **Fig. S4C** but with
327 smaller sample sizes and without using a strict mean fluorescence intensity (MFI)-based cutoff, was
328 previously published (21). Although combined day 28 AIM and AIM+ICS data was published to show T
329 cell response rates between the treatment and placebo groups (21), it was not presented as longitudinal
330 data (as shown in Fig. **4A-C**, **S4A**). Day 0 and 7 T cell data have not been previously published.
331

332 ### SARS2 viral RNA

333 Samples were collected, processed, and analyzed as previously reported (47). In brief, nasopharyngeal
334 swab samples were collected by ACTIV-2/A5401 trial staff at designated study sites on assigned study
335 days (days 0, 7, 14, and 28) using standardized swabs and validated collection and storage procedures.
336 nasopharyngeal swabs were frozen upon collection and stored at −80 °C (−65 °C to −95 °C) until shipped
337 on dry ice to a central laboratory (University of Washington) for extraction, amplification and quantitative

338 detection testing using validated, previously published methods using the Abbott m2000sp/rt system with
339 a validated controls and standards for correlation with cycle threshold (Ct) and viral load. The limit of
340 detection (LOD) was 1.4 log10 copies/mL, lower limit of quantification (LLOQ) was 2 log10 copies/mL, and
341 upper limit of quantification (ULOQ) was 7 log10 copies/mL for this assay. For samples with viral RNA
342 levels above the ULOQ, samples were diluted, and the assay repeated to obtain a quantitative value.
343
344 **PBMC and viability-based quality control**
345 Peripheral blood was collected by ACTIV-2/A5401 trial staff at designated study sites on assigned study
346 days. Serum and peripheral blood mononuclear cells (PBMC) for immunologic testing were isolated from
347 whole blood using standard operating procedures. PBMC were cryopreserved and stored in liquid
348 nitrogen until ready for use, then thawed at 37°C, resuspended in warm complete RPMI medium with 5%
349 human AB serum (Gemini Bioproducts) and benzonase and centrifuged to remove cryopreservation
350 medium. Following washing, cell counts were performed, and viability assessed using the Muse Count &
351 Viability Kit (Muse Cell Analyzer; Luminex). A PBMC viability threshold was set at ≥ 75% for all samples for
352 inclusion in data analysis. PBMC with viability below this threshold failed to appropriately respond to
353 control stimuli. Four of 95 PBMC samples failed to meet the viability cutoff and were excluded from
354 analyses. PBMC were resuspended to achieve a final concentration of 100,000 PBMC/100 µL for plating
355 in 96-well format for T cell assays. Cryopreserved convalescent COVID-19 donor PBMC from known
356 positive responders obtained from the Sette lab under an LJI IRB-approved protocol (VD-214) served as
357 batch controls across T cell assays. These PBMC were handled in the same fashion as ACTIV-2/A5401
358 PBMC samples. Additional quality control metrics were also applied, as described below for the individual
359 T cell assays.
360
361 **Activation induced marker assay (AIM)**
362 As previously described (21), PBMC were cultured in 96-well U-bottom plates for 24 hours at 37°C in an
363 incubator with 5% CO_2 in the presence of a single stimulus per well: a negative control (equimolar amount
364 of DMSO vehicle), a positive control (Staphylococcal enterotoxin B at 1 µg/mL), or a single SARS2 MP (1
365 µg/mL per MP) (20, 28, 59) containing Spike (S) (20, 59) or paired SARS2 non-Spike epitope MPs (CD4-RE
366 or CD8-RE dominant and subdominant MPs (28)). The Spike MP was comprised of overlapping peptides
367 spanning the full-length ancestral Spike protein. The CD4-RE pools ("non-Spike") consisted of
368 experimentally validated and optimized class II epitopes from the remainder of the SARS2 proteome
369 (outside of the Spike open reading frame (ORF)). CD8 AIM responses were calculated using the AIM+ICS
370 assay as PBMC counts were limited and did not allow for CD8-RE MP wells to be plated for both AIM and
371 AIM+ICS assays (see AIM+ICS assay section below for additional experimental details).
372 PBMC were plated at 1 x 10^6 PBMC per MP stimulation well and between 0.5-1 x 10^6 PBMC per
373 control well; negative controls were plated in duplicate. Prior to stimulation, PBMC were incubated at 37°C
374 for 15 minutes with 0.5 µg/mL anti-human CD40 blocking antibody (Miltenyi Biotec) per well. Chemokine
375 receptor antibodies were also added to each well on day 1 (see ref 21 for antibodies used in the AIM
376 assay). After a 24-hour incubation, the plates were centrifuged, cells washed with PBS, then stained with
377 LIVE/DEAD Fixable Blue (Invitrogen) 1:1000 in PBS with Fc block (5 µL/sample; BD Biosciences (BD)) for
378 15 minutes at room temperature, washed with FACS buffer (3% FBS in DPBS without calcium or

379 magnesium), surface stained (see ref 21 for surface staining panel; 30 minutes at 4°C), fixed with BD Cytofix
380 Fixation Buffer (4°C for 20 minutes), and stored at 4°C (up to overnight) until flow cytometric analysis was
381 performed using a 5-laser Cytek Aurora (Cytek Biosciences). Flow cytometric data was acquired separately
382 for each sample and stimulation condition; no samples were pooled. Analysis was performed using FlowJo
383 (BD), and AIM^+ gates were drawn based on MP-stimulated responses relative to negative (DMSO) and
384 positive (SEB) controls. T cell assays on two SARS2 convalescent control PBMC samples were run with each
385 set of experimental PBMC samples to account for batch effects; aliquots from the same PBMC controls
386 were used across batches. A single gating strategy was applied to all samples across all batches unless
387 there was a clear batch-specific effect to justify modifying the gates for a specific batch of samples. Our
388 standard acceptable background (% AIM^+ T cells) for DMSO gates is 0.1. DMSO gates were set to target
389 average background values $\leq$ 0.1 using the same flow cytometry gating strategy for all samples across all
390 batches. CD4 and CD8 T cell responses to MP versus DMSO stimulation are shown in **Fig. S2K-M** and
391 **S3G-H**. Higher background was allowed for CD8 AIM ($CD69^+41BB^+$) assays (**Fig. S3G**) based on higher
392 background observed for CD8 AIM both here and in prior studies (21). ICS ($CD69^+IFN\gamma^+$) was preferentially
393 used as the main readout for SARS2-specific CD8 T cell responses given lower background (**Fig. S3H**) with
394 comparable response rates to CD8 AIM.
395 PBMC quality was evaluated by measuring the median response to SEB for all samples, and
396 samples with responses <50% of the overall median SEB response were excluded from downstream
397 analyses. Two DMSO negative control well replicates were run for each sample and the average of the
398 individual DMSO wells for each sample was calculated. T cell responses were verified by stimulation index
399 (SI) as a quality control. SI was calculated for each sample as the fold change in responses to MP-stimulation
400 versus the average response to DMSO for the same subject (as shown in **Fig. S2N-P** and **Fig. S3I-J**). An SI
401 cutoff of 2 was used for determining AIM^+ CD4 T cell responses and 3 for AIM^+ CD8 T cell responses. The
402 higher SI cutoff for CD8 T cell responses was applied based on higher background for CD8 AIM assays.
403 When a non-zero DMSO value was needed for calculating the stimulation index, the minimum DMSO
404 signal was set to 0.005%. For each MP-stimulated sample, the average DMSO value was subtracted from
405 the MP response to calculate the background subtracted MP response. Background subtracted S and non-
406 S values are shown for all figures. Combined AIM responses were calculated as the mathematical sum of
407 the background subtracted responses to individual (S plus non-S) MPs. In the case of negative AIM
408 responses to both S and non-S megapools, or summative responses that were less than the lower limit of
409 quantitation (LOQ) for the assay, as described below, the combined AIM response was also considered
410 negative. The geometric mean of all DMSO control wells for all samples for each assay was calculated to
411 determine the LOQ for the assay. Positive responders were defined as those with background subtracted
412 responses greater than the LOQ. The baseline for the y-axis was set to 0.5 x LOQ. All non-responders
413 were set to this baseline.
414

415 **Hybrid activation induced marker plus intracellular cytokine staining assay (AIM+ICS)**

416 AIM+ICS assays were also performed as previously described (21). For CD4 T cells, intracellular cytokine
417 expression was measured in conjunction with surface CD40L. For CD8 T cells, intracellular cytokine staining
418 was measured in conjunction with surface CD69. PBMC were thawed and plated in parallel and as AIM
419 assays but with the addition of wells for CD8-RE MP (paired dominant and non-dominant epitopes (28))

420 stimulation. The CD8-RE pools ("non-Spike") consisted of optimized, experimentally validated class I
421 epitopes from the remainder of the SARS2 proteome (outside of the Spike ORF) (28). Cells were incubated
422 with anti-CD40 blocking antibody as for AIM assays, but no chemokine receptor antibodies were added
423 on day 1 except for CXCR5 for identification of circulating T_{FH} cells (see ref 21 for antibodies used). After
424 20-22 hours, PMA (0.05 µg/mL) and ionomycin (0.25 µg/mL) were added to the positive (ICS) control wells.
425 Two hours later, 0.25 µL/well of GolgiStop (BD) and GolgiPlug (BD) and the AIM marker antibodies (see
426 ref(21)) were added to all samples, and the plates were incubated for another 4 hours at 37°C (in a 5%
427 CO_2 incubator). Cells were then washed, surface stained for 30 minutes at 4°C, fixed and washed using
428 Cytofix/Cytoperm (BD) per the manufacturers' protocol. Intracellular cytokine staining was then performed
429 using antibodies diluted in Perm/Wash Buffer (BD) for 30 minutes at 4°C. Cells were washed with Stain
430 Buffer with FCS (BD) and stored in this buffer at 4°C until flow cytometric analysis was performed using a
431 Cytek Aurora. Flow cytometric data was acquired separately for each sample and stimulation condition.
432 Gating and quality control evaluations with SEB responses and SI calculations were performed as
433 described above for AIM assays. PMA + ionomycin served as an additional control for cytokine production
434 (ICS). For each MP-stimulated sample, the average DMSO value was subtracted from the MP response to
435 calculate the background subtracted MP response. Background subtracted values are shown for all figures
436 unless indicated. Combined responses were calculated as the sum of the background subtracted
437 responses to individual MPs (S and CD4-RE for CD4 T cells, S and CD8-RE for CD8 T cells). In the case of
438 negative ICS responses to both S and non-S MPs, the combined response was also considered negative.
439 The LOQ and baseline was calculated and plotted as described above for AIM assays.
440

441 **Binding antibody titers**

442 Serum SARS2-specific binding antibody assays were performed using the Bio-Plex Pro Human SARS2 IgG
443 4-Plex Panel serology assay (Bio-Rad 12014634) according to the manufacturer's protocol, as previously
444 described (21). MFI-based cutoffs for seropositivity are indicated in the figures.
445

446 **Pseudovirus neutralizing antibody titers**

447 Half-maximal neutralizing antibody titers (NT50) were generated using a lentiviral pseudovirus assay, as
448 previously described (60). Briefly, PSV was generated in HEK293T cells co-transfected with SARS2 Spike
449 expression and pNL4–3.luc.R-E-mCherry-luciferase reporter packaging plasmids. Serum was isolated from
450 the peripheral blood of study subjects using standard protocols, frozen and shipped to the testing site
451 without thawing until ready for use. The serum was then serially diluted and incubated with SARS2 PSV,
452 then HEK293T cells stably expressing human angiotensin converting enzyme 2. Serum dilutions were run
453 in triplicate. The percent inhibition was calculated using relative light units emitted by the reporter at each
454 dilution and plotted versus the log serum dilution. The NT50 was then derived by non-linear regression.
455 The limit of detection for the assay was defined by the lowest dilution tested (1:3) as indicated in figures.
456

457 **Statistics**

458 Statistical analyses were performed in GraphPad Prism 10 (GraphPad Software) and Microsoft Excel.
459 Comparisons of SARS2-specific T cell response magnitudes and antibody titers between treatment and

placebo groups for equivalent conditions were determined by Mann-Whitney tests. Fisher's exact tests were used to compare participant characteristics (**Fig. 1A**) and to compare SARS2-specific T cell positive and negative response rates between treatment and control groups. Kruskal-Wallis nonparametric tests with post-hoc Dunn's multiple comparison tests were used for assessing T cell responses across more than one stimulation condition or cell type. Relationships between SARS2 nasopharyngeal RNA levels and immune responses were assessed using nonparametric Spearman correlations. One-way ANCOVA were performed on unadjusted viral RNA and immune response data to determine if the relationships between SARS2 NP RNA levels and SARS2-specific T cell responses at study day 0 were dependent on SARS2 nAb serostatus (**Fig. S5M-O**).

Individual variation in days from symptom onset to study entry (day 0) was accounted for using a log-linear regression model (**Fig. S7A-E**). Adjusted SARS2 NP RNA levels (**Fig. S7A**) and adaptive immune responses (log_{10} transformed CD4 T cell responses, CD8 T cell responses, and nAb titers; **Fig. S7B-E**) at 6 days post-symptom onset (the median time from symptom onset at study entry) were calculated for all participants using the linear regression models shown in **Fig. S7A-E** to adjust the data shown in **Fig. 5A-D**. Data from five individuals were excluded from this analysis as outliers as these individuals had undetectable viral RNA on study day 0 but were reportedly 4-5 days PSO as study entry. This included four values from individuals who consistently tested negative for viral RNA (from both nasal and NP swabs) on all study days, and a value for one individual who tested negative for viral NP RNA on study day 0 but who subsequently tested positive for viral NP RNA on study days 3, 7, and 14. The adjusted NP viral RNA and adaptive immunity data was plotted and analyzed using nonparametric Spearman correlations to be able to compare the original (unadjusted) data (**Fig. Fig. 5A-D**) to the adjusted data (**Fig. S7F-I**) using the same correlation method.

For all analyses, a two-sided 5% type I error rate was used, without adjustment for multiple comparisons, except as noted above. Additional details can be found in the results, figures and corresponding legends.

Study approval

The ACTIV-2/A5401 clinical trial protocol (ClinicalTrials.gov Identifier: NCT04518410) was approved by a central institutional review board (IRB); Advarra (Pro00045266). The La Jolla Institute for Immunology (LJI) IRB provided additional oversight for this study. All individuals enrolled in ACTIV-2/A5401 provided written informed consent for participation.

Data availability

The authors confirm that the source data underlying the findings are fully available. Due to ethical restrictions, additional ACTIV-2/A5401 clinical trial study data beyond what is presented in this manuscript and supplement are available upon request from the AIDS Clinical Trials Group (ACTG) and with the written agreement of ACTG and the manufacturer of the investigational product. Completion of a data use agreement may be required. Values for all data points in graphs are reported in the Supporting Data Values file.

AUTHOR CONTRIBUTIONS

Conceptualization, S.I.R., D.M.S., and S.C.; Investigation, S.I.R., P.G.L., F.F., A.H.; Formal Analysis, S.I.R., B.P, S.C.; Patient Recruitment and Samples D.M.S.; Material Resources, A.G., D.W., P.K., A.S.; Writing, S.I.R., F.F., D.M.S. and S.C.; Supervision D.M.S. and S.C.

FUNDING

This work was supported in part by the National Institute of Allergy and Infectious diseases (NIAID) of the National Institutes of Health (NIH), Department of Health and Human Services, under contract no. 75N93019C00065 (A.S, D.W.), under awards AI036214, AI131385, UM1AI068634, UM1AI068636, and UM1AI106701. Additional support was provided in part by the John and Mary Tu Foundation, NIH T32 AI007036 (S.I.R.) and an A.P. Giannini Foundation fellowship award (S.I.R.). Bamlanivimab was donated by Eli Lilly and Company. The content presented is the sole responsibility of the authors and may not represent the opinions of the NIH.

ACKNOWLEDGMENTS

We would like to thank the study participants, site staff and investigators, members of the study team and community advisory board, the AIDS Clinical Trials Group (ACTG), the Harvard Center for Biostatistics in AIDS Research (CBAR) and ACTG Statistical and Data Analysis Center (SDAC), the National Institute of Allergy and Infectious Diseases (NIAID) / Division of AIDS (DAIDS), Bill Erhardt, the Accelerating COVID-19 Therapeutic Interventions and Vaccines (ACTIV) partnership, and PPD for making this study possible. See Supplemental Acknowledgments for additional details.

REFERENCES

1. Gilbert PB, et al. Immune correlates analysis of the mRNA-1273 COVID-19 vaccine efficacy clinical trial. *Science*. 2022;375(6576):43–50.

2. Corbett KS, et al. Immune correlates of protection by mRNA-1273 vaccine against SARS-CoV-2 in nonhuman primates. *Science*. 2021;373(6561):eabj0299.

3. Feng S, et al. Correlates of protection against symptomatic and asymptomatic SARS-CoV-2 infection. *Nat Med*. 2021;27(11):2032–2040.

4. Gilbert PB, et al. A Covid-19 Milestone Attained — A Correlate of Protection for Vaccines. *N Engl J Med*. 2022;387(24):2203–2206.

5. Fong Y, et al. Immune correlates analysis of the PREVENT-19 COVID-19 vaccine efficacy clinical trial. *Nat Commun*. 2023;14(1):331.

6. Fong Y, et al. Immune correlates analysis of the ENSEMBLE single Ad26.COV2.S dose vaccine efficacy clinical trial. *Nat Microbiol*. 2022;7(12):1996–2010.

7. Regev-Yochay G, et al. Correlates of protection against COVID-19 infection and intensity of symptomatic disease in vaccinated individuals exposed to SARS-CoV-2 in households in Israel (ICoFS): a prospective cohort study. *The Lancet Microbe*. 2023;4(5):e309–e318.

8. Hertz T, et al. Correlates of protection for booster doses of the SARS-CoV-2 vaccine BNT162b2. *Nat Commun*. 2023;14(1):4575.

9. Stadler E, et al. Monoclonal antibody levels and protection from COVID-19. *Nat Commun*. 2023;14(1):4545.

10. Levin MJ, et al. Intramuscular AZD7442 (Tixagevimab–Cilgavimab) for Prevention of Covid-19. *N Engl J Med*. 2022;386(23):2188–2200.

11. Isa F, et al. Repeat subcutaneous administration of casirivimab and imdevimab in adults is well-tolerated and prevents the occurrence of COVID-19. *International Journal of Infectious Diseases*. 2022;122:585–592.

12. O'Brien MP, et al. Subcutaneous REGEN-COV Antibody Combination to Prevent Covid-19. *N Engl J Med*. 2021;385(13):1184–1195.

13. Wilkinson TM, et al. Preexisting influenza-specific CD4+ T cells correlate with disease protection against influenza challenge in humans. *Nat Med*. 2012;18(2):274–280.

14. Sette A, Crotty S. Adaptive immunity to SARS-CoV-2 and COVID-19. *Cell*. 2021;184(4):861–880.

15. Follmann D, et al. Examining protective effects of SARS-CoV-2 neutralizing antibodies after vaccination or monoclonal antibody administration. *Nat Commun*. 2023;14(1):3605.

16. Goldblatt D, et al. Correlates of protection against SARS-CoV-2 infection and COVID-19 disease. *Immunol Rev*. 2022;310(1):6–26.

574 17. Sette A, Sidney J, Crotty S. T Cell Responses to SARS-CoV-2. *Annu Rev Immunol*. 2023;41(1):343–
575 373.

576 18. Rydyznski Moderbacher C, et al. Antigen-Specific Adaptive Immunity to SARS-CoV-2 in Acute
577 COVID-19 and Associations with Age and Disease Severity. *Cell*. [published online ahead of print: 2020].
578 https://doi.org/10.1016/j.cell.2020.09.038.

579 19. Dan JM, et al. Immunological memory to SARS-CoV-2 assessed for up to 8 months after infection.
580 *Science*. 2021;371(6529). https://doi.org/10.1126/science.abf4063.

581 20. Grifoni A, et al. Targets of T Cell Responses to SARS-CoV-2 Coronavirus in Humans with COVID-19
582 Disease and Unexposed Individuals. *Cell*. 2020;181(7):1489-1501.e15.

583 21. Ramirez SI, et al. Bamlanivimab therapy for acute COVID-19 does not blunt SARS-CoV-2–specific
584 memory T cell responses. *JCI Insight*. 2022;7(24):e163471.

585 22. Weiskopf D, et al. Phenotype and kinetics of SARS-CoV-2–specific T cells in COVID-19 patients with
586 acute respiratory distress syndrome. *Sci Immunol*. 2020;5(48):eabd2071.

587 23. Notarbartolo S, et al. Integrated longitudinal immunophenotypic, transcriptional and repertoire
588 analyses delineate immune responses in COVID-19 patients. *Sci Immunol*. 2021;6(62):eabg5021.

589 24. Gao Y, et al. Ancestral SARS-CoV-2-specific T cells cross-recognize the Omicron variant. *Nat Med*.
590 2022;28(3):472–476.

591 25. Zhang Z, et al. Humoral and cellular immune memory to four COVID-19 vaccines. *Cell*.
592 2022;185(14):2434-2451.e17.

593 26. Mateus J, et al. Low-dose mRNA-1273 COVID-19 vaccine generates durable memory enhanced by
594 cross-reactive T cells. *Science*. 2021;374(6566):eabj9853.

595 27. Rydyznski Moderbacher C, et al. NVX-CoV2373 vaccination induces functional SARS-CoV-2-specific
596 CD4+ and CD8+ T cell responses. *J Clin Invest*. 2022;132(19):e160898.

597 28. Yu ED, et al. Development of a T cell-based immunodiagnostic system to effectively distinguish
598 SARS-CoV-2 infection and COVID-19 vaccination status. *Cell Host & Microbe*. 2022;30(3):388-399.e3.

599 29. Tarke A, et al. SARS-CoV-2 vaccination induces immunological T cell memory able to cross-recognize
600 variants from Alpha to Omicron. *Cell*. 2022;185(5):847-859.e11.

601 30. Wherry EJ, Barouch DH. T cell immunity to COVID-19 vaccines. *Science*. 2022;377(6608):821–822.

602 31. Sahin U, et al. BNT162b2 vaccine induces neutralizing antibodies and poly-specific T cells in humans.
603 *Nature*. 2021;595(7868):572–577.

604 32. Müller TR, et al. Additive effects of booster mRNA vaccination and SARS-CoV-2 Omicron infection on
605 T cell immunity across immunocompromised states. *Sci Transl Med*. 2023;15(704):eadg9452.

606 33. Sette A, Crotty S. Immunological memory to SARS-CoV-2 infection and COVID-19 vaccines.
607 *Immunological Reviews*. 2022;310(1):27–46.

608 34. Moss P. The T cell immune response against SARS-CoV-2. *Nat Immunol*. 2022;23(2):186–193.

609 35. Bertoletti A, et al. SARS-CoV-2-specific T cells in infection and vaccination. *Cell Mol Immunol*.
610 2021;18(10):2307–2312.

611 36. Wagstaffe HR, et al. Mucosal and systemic immune correlates of viral control after SARS-CoV-2
612 infection challenge in seronegative adults. *Sci Immunol*. 2024;9(92):eadj9285.

613 37. Tan AT, et al. Early induction of functional SARS-CoV-2-specific T cells associates with rapid viral
614 clearance and mild disease in COVID-19 patients. *Cell Reports*. 2021;34(6):108728.

615 38. Swadling L, et al. Pre-existing polymerase-specific T cells expand in abortive seronegative SARS-
616 CoV-2. *Nature*. 2022;601(7891):110–117.

617 39. Rydyznski Moderbacher C, et al. Antigen-Specific Adaptive Immunity to SARS-CoV-2 in Acute
618 COVID-19 and Associations with Age and Disease Severity. *Cell*. 2020;183(4):996-1012.e19.

619 40. Eser TM, et al. Nucleocapsid-specific T cell responses associate with control of SARS-CoV-2 in the
620 upper airways before seroconversion. *Nat Commun*. 2023;14(1):2952.

621 41. Koutsakos M, et al. SARS-CoV-2 breakthrough infection induces rapid memory and de novo T cell
622 responses. *Immunity*. 2023;56(4):879-892.e4.

623 42. Painter MM, et al. Prior vaccination promotes early activation of memory T cells and enhances
624 immune responses during SARS-CoV-2 breakthrough infection. *Nat Immunol*. 2023;24(10):1711–1724.

625 43. Arieta CM, et al. The T-cell-directed vaccine BNT162b4 encoding conserved non-spike antigens
626 protects animals from severe SARS-CoV-2 infection. *Cell*. 2023;186(11):2392-2409.e21.

627 44. Tai W, et al. An mRNA-based T-cell-inducing antigen strengthens COVID-19 vaccine against SARS-
628 CoV-2 variants. *Nat Commun*. 2023;14(1):2962.

629 45. Sette A, Saphire EO. Inducing broad-based immunity against viruses with pandemic potential.
630 *Immunity*. 2022;55(5):738–748.

631 46. Kingstad-Bakke B, et al. Vaccine-induced systemic and mucosal T cell immunity to SARS-CoV-2 viral
632 variants. *Proc Natl Acad Sci USA*. 2022;119(20):e2118312119.

633 47. Chew KW, et al. Antiviral and clinical activity of bamlanivimab in a randomized trial of non-
634 hospitalized adults with COVID-19. *Nat Commun*. 2022;13(1):4931.

635 48. Puhach O, Meyer B, Eckerle I. SARS-CoV-2 viral load and shedding kinetics. *Nat Rev Microbiol*.
636 [published online ahead of print: December 2, 2022]. https://doi.org/10.1038/s41579-022-00822-w.

637 49. Killingley B, et al. Safety, tolerability and viral kinetics during SARS-CoV-2 human challenge in young
638 adults. *Nat Med*. 2022;28(5):1031–1041.

639 50. Chen P, et al. SARS-CoV-2 Neutralizing Antibody LY-CoV555 in Outpatients with Covid-19. *N Engl J*
640 *Med*. 2021;384(3):229–237.

641 51. Crotty S. T Follicular Helper Cell Biology: A Decade of Discovery and Diseases. *Immunity*.
642 2019;50(5):1132–1148.

643 52. Lederer K, et al. Germinal center responses to SARS-CoV-2 mRNA vaccines in healthy and
644 immunocompromised individuals. *Cell*. 2022;185(6):1008-1024.e15.

645 53. Tarke A, et al. Comprehensive analysis of T cell immunodominance and immunoprevalence of SARS-
646 CoV-2 epitopes in COVID-19 cases. *Cell Reports Medicine*. 2021;2(2):100204.

647 54. Mateus J, et al. Selective and cross-reactive SARS-CoV-2 T cell epitopes in unexposed humans.
648 *Science*. 2020;370(6512):89–94.

649 55. Lindeboom RGH, et al. Human SARS-CoV-2 challenge uncovers local and systemic response
650 dynamics. *Nature*. 2024;631(8019):189–198.

651 56. Ramirez SI, et al. Immunological memory diversity in the human upper airway. *Nature*.
652 2024;632(8025):630–636.

653 57. Bhavsar D, et al. Mucosal antibody responses to SARS-CoV-2 booster vaccination and breakthrough
654 infection. *mBio*. 2023;14(6):e02280-23.

655 58. Cai C, et al. SARS-CoV-2 vaccination enhances the effector qualities of spike-specific T cells induced
656 by COVID-19. *Sci Immunol*. 2023;8(90):eadh0687.

657 59. Grifoni A, et al. SARS-CoV-2 human T cell epitopes: Adaptive immune response against COVID-19.
658 *Cell Host and Microbe*. 2021;29(7):1076–1092.

659 60. Heaps AL, et al. Rapid determination of SARS-CoV-2 antibody neutralization titer using Bio-Rad Bio-
660 Plex correlates strongly with pseudovirus-determined neutralization titer. *Journal of Virological Methods*.
661 2023;316:114726.

A

	Treatment (n = 46)	Placebo (n = 49)	p-value
Age (yrs) Range [Median, IQR]	18-86 [46, 22]	19-72 [43, 20.5]	0.45
Sex, n (%)			0.41
Male	27 (59%)	24 (49%)	
Female	19 (40%)	25 (51%)	
Race, n (%)			0.59
African American or Black	7 (15%)	5 (10%)	
Alaskan Native/American Indian	1 (2%)	0 (0%)	
Asian	1 (2%)	3 (6%)	
Native Hawaiian/Pacific Islander	0 (0%)	0 (0%)	
Other/Mixed Race	1 (2%)	3 (6%)	
Unknown	0 (0%)	1 (2%)	
White	36 (78%)	37 (76%)	
Ethnicity, n (%)			0.09
Hispanic	6 (13%)	12 (24%)	
Non-Hispanic	42 (87%)	35 (65%)	
Unknown	0 (0%)	2 (4%)	
Sample Collection Dates	Oct-Nov 2020	Oct-Nov 2020	n.a.
SARS-CoV-2 PCR Positivity	46 (100%)	49 (100%)	n.a.
Vaccination status, n (%)			n.a.
Vaccinated at study day 0	0 (0%)	0 (0%)	
Vaccinated by study day 28	0 (0%)	0 (0%)	
Risk for severe COVID-19, n (%)			0.84
High risk for progression	24 (52%)	24 (49%)	
Low risk for progression	22 (48%)	25 (51%)	

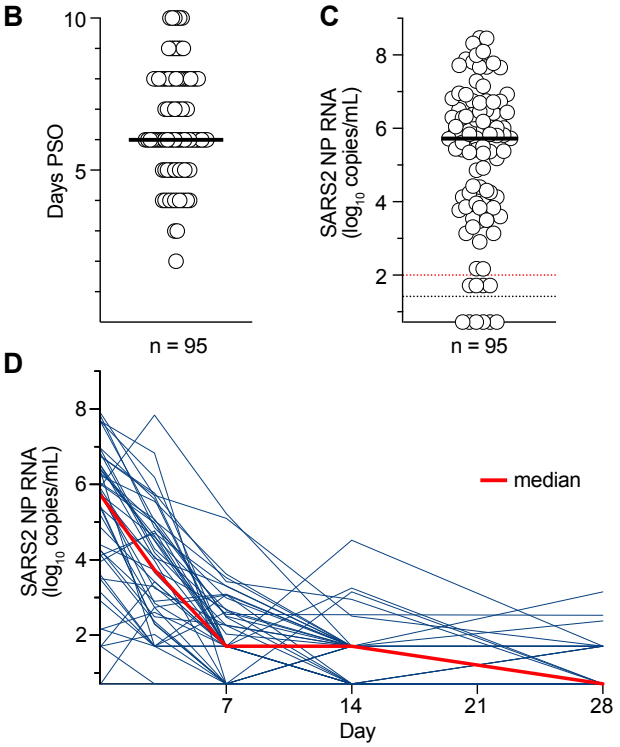

Figure 1. Study cohort characteristics and SARS2 NP RNA levels during acute COVID-19 and longitudinally.
A. Demographics and other pertinent characteristics of the matched bamlanivimab (Treatment) and placebo group participants included in this study. Total n = 95 subjects. See methods for additional details. **B.** Median days post-symptom onset (PSO) from start of COVID-19 symptoms to study entry (study day 0) for all participants. **C.** SARS-CoV-2 NP RNA by quantitative reverse transcription polymerase chain reaction (RT-qPCR) for all participants prior to treatment on study day 0. Dotted black line limit of detection (LOD). Dotted red line limit of quantification (LOQ). Values >LOQ were considered positive. Bar = median. **D.** Longitudinal SARS-CoV-2 NP RNA data for the placebo group (n = 49) for study days 0, 7, 14, and 28. Median for each time point in red.

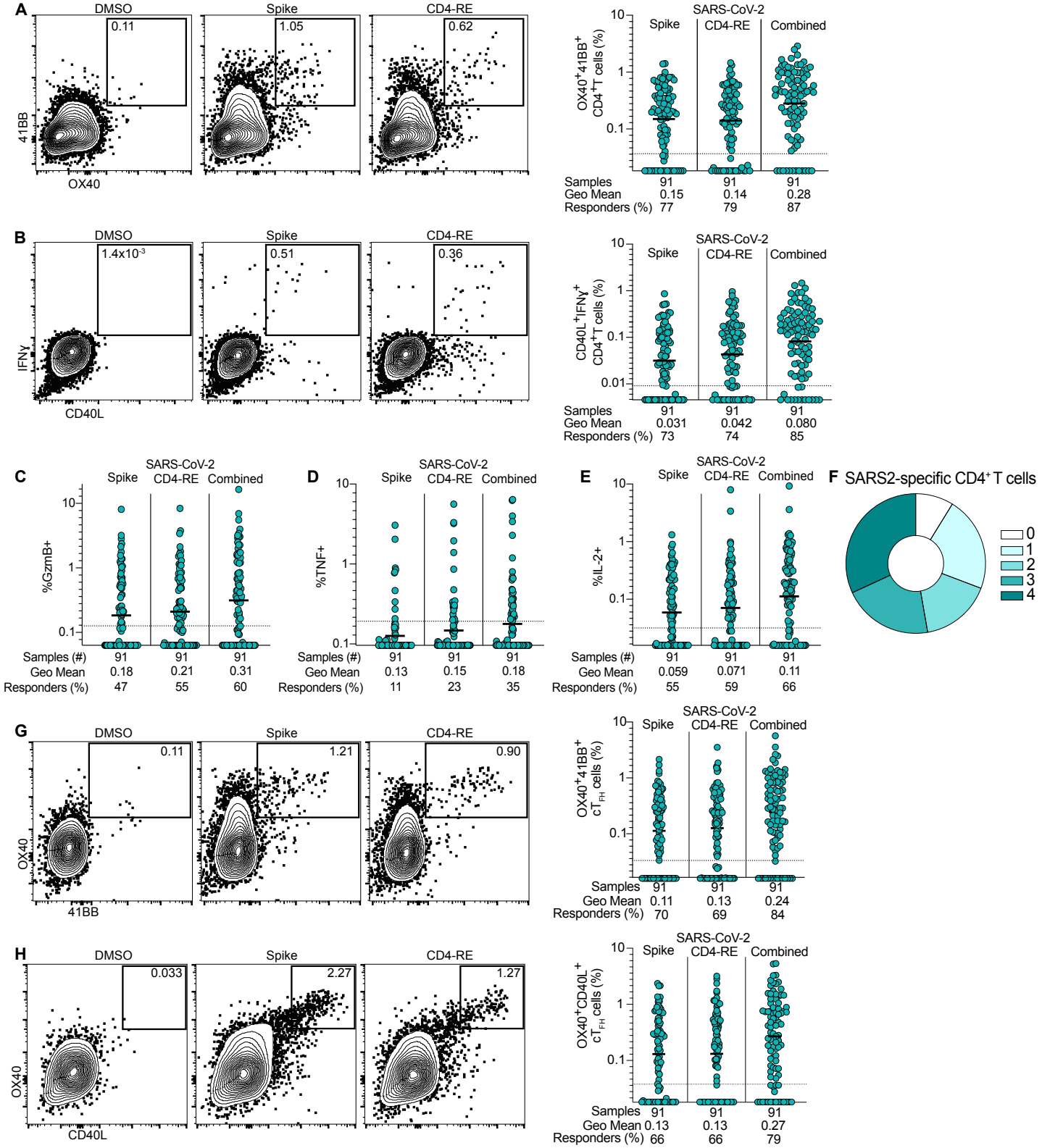

Figure 2. Antigen-specific CD4 T cell responses to primary SARS2 infection and acute COVID-19.

A-B. Representative flow cytometry plots and frequency of SARS2-specific CD4 T cells to DMSO (negative control), Spike and CD4-RE MP stimulation conditions (Combined = sum of Spike + CD4-RE responses; see Methods for additional details) by (**A**) AIM using surface OX40 and 41BB co-expression, and (**B**) IFNγ ICS among surface CD40L$^+$ cells. **C-E.** Study day 0 SARS2-specific CD4 T cell intracellular cytokine production (**C**) GzmB, (**D**) TNF, or (**E**) IL-2 among surface CD40L$^+$ cells. **F.** Parts of a whole donut plot summary of intracellular cytokine (IFNγ, GzmB, TNF, IL-2) production by SARS2-specific CD4 T cells expressing 0 to 4 cytokines. **G-H.** As in **A** and **Fig. S2B** but for SARS2-specific circulating T_{FH} (cT_{FH}) cells. Bars = geometric mean. Dotted lines = LOQ. Flow cytometry gates display frequency (%).

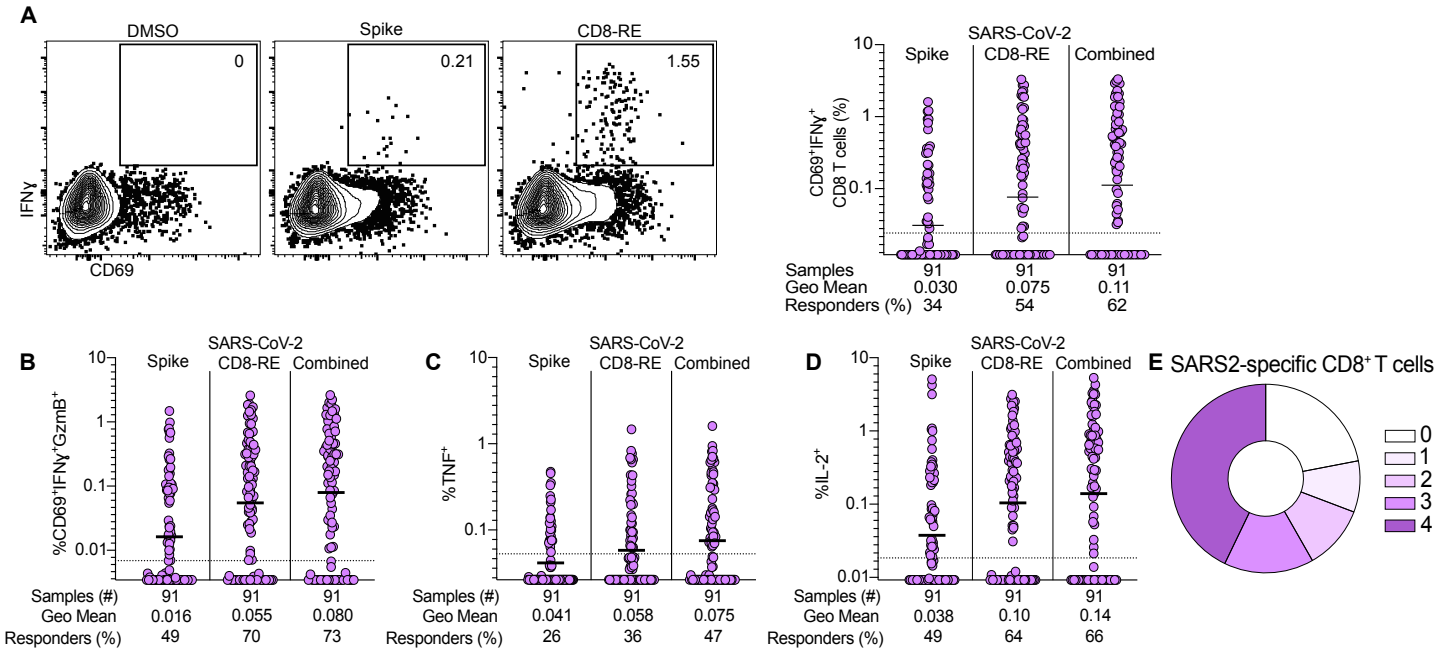

Figure 3. Antigen-specific CD8 T cell responses to primary SARS2 infection and acute COVID-19.

A. Representative flow cytometry plots and frequency of SARS2-specific CD8 T cells to DMSO (negative control), Spike and CD8-RE MP stimulation conditions (Combined = sum of Spike + CD8-RE responses; see Methods for additional details) by IFNγ+ ICS among CD69+ cells. **B-D.** (**B**) IFNγ and GzmB, (**C**) TNF, (**D**) IL-2 production. **E.** Parts of a whole donut plot summary of intracellular cytokine (IFNγ, GzmB, TNF, IL-2) production by SARS2-specific CD8 T cells expressing 0 to 4 cytokines. Bars = geometric mean. Dotted lines = LOQ. Flow cytometry gates display frequency (%).

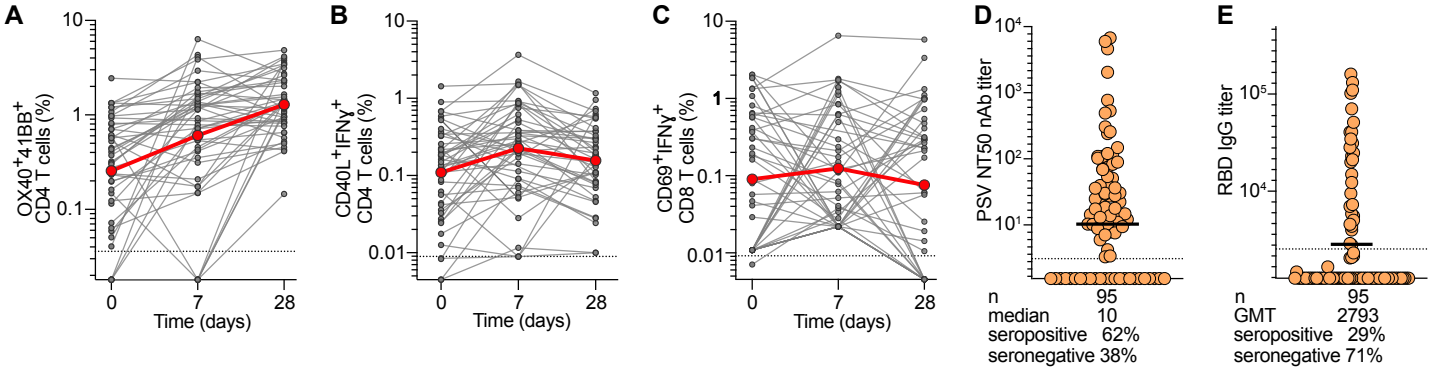

Figure 4. Longitudinal SARS2-specific T cell responses and Ab responses to primary SARS2 infection and acute COVID-19.
A-C. Longitudinal combined (Spike plus non-Spike) (**A**) CD4 AIM (**B**) CD4 AIM+ICS, (**C**) CD8 IFNγ+ T cell responses in placebo group (n = 49) participants at study days 0, 7, and 28. Red dots and lines represent median. Dotted line = LOQ. **D.** Study day 0 pre-treatment nAb titers for all participants. Dotted black line indicates LOD; seropositivity defined by values >LOD. Bar is median. **E.** Study day 0 pre-treatment RBD IgG binding titers for all participants. Dotted black line indicates cut off for seropositivity. Bar is geometric mean titer (GMT).

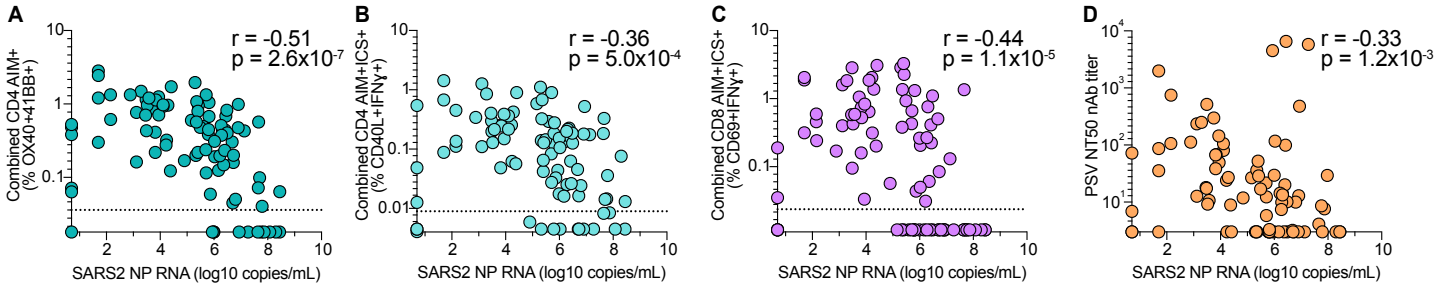

Figure 5. Correlative relationships between SARS2-specific adaptive immunity and upper airway viral RNA in acute COVID-19.
A-D. Relationships between study day 0 SARS2 NP RNA and combined day 0 SARS2-specific T cell responses by (**A**) CD4 AIM$^+$, (**B**) CD4 IFNγ, (**C**) CD8 IFNγ$^+$ and (**D**) nAb titers.